

**Fermi-surface effect on magnetic interlayer coupling**

Erik Holmström,\* Anders Bergman, and Lars Nordström

*Condensed Matter Theory Group, Physics Department, Uppsala University, S-75121 Uppsala, Sweden*

I. A. Abrikosov

*Department of Physics and Measurement Technology, Linköping University, Linköping SE-58183, Sweden*

S. B. Dugdale and B. L. Györfy

*H.H. Wills Physics Laboratory, University of Bristol, Tyndall Avenue, BS8 1TL, Bristol, United Kingdom*

(Received 26 January 2004; revised manuscript received 27 April 2004; published 10 August 2004)

The oscillating magnetic interlayer coupling of Fe over spacer layers consisting of  $\text{Cu}_x\text{Pd}_{1-x}$  alloys is investigated by first principles density functional theory. The amplitude, period, and phase of the coupling, as well as the disorder-induced decay, are analyzed in detail and the consistency to the Ruderman-Kittel-Kasuya-Yoshida theory is discussed. An effect of the Fermi surface nesting strength on the amplitude is established from first principles calculations. An unexpected variation of the phase and disorder-induced decay is obtained and the results are discussed in terms of asymptotics.

DOI: 10.1103/PhysRevB.70.064408

PACS number(s): 75.70.Cn, 75.30.Et, 75.50.Ss

**I. INTRODUCTION**

An interesting feature of random substitutional metallic alloys is their rapidly but smoothly changing Fermi surfaces as the electron per atom ratio,  $e/a$ , varies with concentration. Such Fermi surface evolution can give rise to dramatic physical phenomena like spin- and charge-density waves or compositional ordering,<sup>1</sup> to mention but a few.

A well-studied effect which is directly governed by the Fermi surface is the magnetic interlayer coupling (MIC) between two magnetic layers across a paramagnetic spacer as the spacer thickness is varied. Many studies exist that confirm the role of the Fermi surface of the spacer as mainly governing the coupling, both experimental<sup>2-4</sup> and theoretical.<sup>5-9</sup> The description of the MIC is thus well developed in the cases of both pure metal and random substitutional metallic alloy spacers and the physical effect that is responsible for the effect is understood to be spin dependent confined electronic states in the spacer. The common models are the so called Ruderman-Kittel-Kasuya-Yoshida (RKKY) model<sup>10,11</sup> and the quantum well model.<sup>6</sup> The theories predict that among several things, the Fermi surface will play an important role in changing the period, amplitude, phase, and decay of the MIC when the spacer is alloyed. The phase is affected by the type of extremal points on the spacer Fermi surface, which may change with concentration. The period changes since the length of the Fermi surface caliper changes as confirmed by Okuno<sup>12</sup> and Bobo<sup>13</sup> for a  $\text{Co}/\text{Cu}_{1-x}\text{Ni}_x/\text{Co}$  system and investigated theoretically by Lathiotakis.<sup>14-16</sup> Finally, the amplitude of the MIC oscillation is influenced by the change in nesting at the Fermi surface.

In some cases, the amplitude does not change very much when the spacer is alloyed<sup>12,13</sup> but in other alloys and for some growth directions the effect is dramatic.<sup>17-19</sup> In the cases where the amplitude is changed by alloying the spacer, it always becomes smaller with increasing impurity concentration. In the studied materials, the decrease in amplitude is not a nesting effect but a disorder-induced damping of the electronic states in the spacer.

One very interesting case where the Fermi surface nesting could affect the amplitude of the MIC in addition to the disorder broadening is the  $\text{Cu}_x\text{Pd}_{1-x}$  alloy. This system exhibits Fermi surface driven compositional ordering where the nesting of the Fermi surface is responsible for the concentration-dependent peaks observed in x-ray diffuse scattering in the concentration range  $0.5 \leq x \leq 0.6$ .<sup>1,20</sup> Recent experimental studies of the Fermi surface nesting show an exceptionally flat region in the [110] direction in a face-centered-cubic (fcc)  $\text{Cu}_{0.6}\text{Pd}_{0.4}$  random alloy sample.<sup>21</sup> From this observation it is reasonable to believe that the nesting might manifest itself as an increase of the amplitude at this concentration. In this paper we will calculate the MIC of the  $\text{Fe}/\text{Cu}_x\text{Pd}_{1-x}/\text{Fe}$  system as function of  $x$ . We will investigate the variation of the period, amplitude, phase, and disorder-induced decay with concentration for spacer thicknesses up to 22 ML. The nesting effect on the amplitudes will be analyzed in detail and the validity of extracting asymptotic properties from this type of calculations is discussed.

**II. THEORY****A. Definition**

In this paper, the following definition of the MIC was used

$$J(N) = E_{\uparrow\downarrow}^{\text{tot}}(N) - E_{\uparrow\uparrow}^{\text{tot}}(N). \quad (1)$$

Here  $E_{\uparrow\downarrow}^{\text{tot}}$  is the total energy of the system with the total magnetic moment of the Fe layers on one side of the system antiparallel (parallel) to the Fe layers on the other side and  $N$  the number of atomic monolayers in the spacer.

In all calculations we used the Korringa-Kohn-Rostocker (KKR)<sup>22</sup> method within the frozen core and atomic-sphere approximations together with the local spin density approximation as parameterized in Ref. 23. To carry out the multilayer calculations, the interface Green's function tech-

nique developed by Skriver and Rosengaard<sup>24</sup> was used. The bulk alloys as well as the layered alloys were treated within the coherent potential approximation (CPA).<sup>25–27</sup>

An advantage of the Green's function technique is that it ensures a correct description of the loss of translational symmetry perpendicular to the interface without the use of an artificial slab or supercell geometry. The multilayer systems consisted of self-consistently calculated bulk potentials for fcc Fe as boundary conditions to the left and right of the multilayer region that consisted of the alloy spacer and some Fe layers that were included in the self-consistent calculation. The spin alignment of the two sides was either parallel or antiparallel. The spacer material was a disordered binary alloy of the form  $\text{Cu}_x\text{Pd}_{1-x}$  for  $x=0.4-0.9$ . The calculations were converged up to an energy difference of  $0.1 \mu\text{Ry}$  between iterations. The  $k$ -point sampling convergence was checked, and we used 1024  $k$  points in the irreducible part of the two-dimensional Brillouin zone. The bulk, as well as the multilayer calculations were calculated in an ideal fcc lattice with the lattice parameter linearly interpolated between Cu and Pd for each concentration. This means that the fcc Fe boundary conditions were recalculated for every Cu concentration that was going to be used in the slab in order to adapt to the global volume change. The choice of fcc Fe in the structure is purely technical in order to optimize the speed of the calculations. A more realistic system would be embedded, thin fcc Fe layers in the alloy but that choice would demand calculations that include more atomic layers and our investigation would become intractable. The MIC should, however, not be qualitatively affected by our choice of semi-infinite fcc Fe as boundary conditions since the properties of the MIC are mainly dictated by the spacer material.

All our calculations were performed scalar relativistically and the detailed form of the Fermi surfaces may have changed if the calculations would have included spin-orbit coupling. However, by comparing our bulk calculations of extremal Fermi surface vectors and shapes of the Fermi surfaces to the fully relativistic calculations and experiments in Refs. 21 and 28, we conclude that the error from the scalar relativistic approximation is small.

## B. Model

The strength of a total energy calculation is that the MIC is obtained directly from the independently calculated energies for each magnetic configuration by using the definition. To gain physical insight, however, we need to consider a model for the MIC. A good choice in this case is to look at the RKKY model for a simple, symmetric quantum well potential but for a general Fermi surface. Such a case is described in detail by Bruno and Stiles<sup>5,6</sup> where the final result in the asymptotic limit ( $\infty$ ) can be written as

$$J_\infty(N) = \sum_i - \left[ \frac{\hbar}{2\pi^2} \kappa_i v_i |\Delta R|^2 \right] \frac{\cos(2Q_i N + \phi_i)}{N^2}. \quad (2)$$

Here, the sum is over the stationary points of the Fermi surface and  $Q_i$  are the vectors on the Fermi surface that connects the extremal points.  $N$  is the thickness of the spacer defined as number of monolayers and  $\phi_i$  is the phase. The

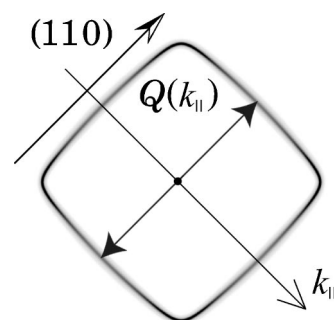


FIG. 1. A cut of the  $\text{Cu}_{0.7}\text{Pd}_{0.3}$  Fermi surface in the  $k_z=0$  plane. The nesting area is clearly visible at this concentration. The spanning vector  $Q$  is displayed together with the direction of growth ( $[110]$ ) and the definition of  $k_{\parallel}$ . The “fuzziness” of the surface represents the half-width of the Bloch spectral function displayed in Fig. 2.

generalized Fermi surface radii  $\kappa_i$  are defined as

$$\kappa_i = \left[ \sqrt{\frac{\partial^2 Q_i(k_{\parallel})}{\partial k_x^2} \frac{\partial^2 Q_i(k_{\parallel})}{\partial k_y^2} - \left( \frac{\partial^2 Q_i(k_{\parallel})}{\partial k_x \partial k_y} \right)^2} \right]^{-1} \quad (3)$$

and  $v_i$  are the reduced Fermi velocities.  $\Delta R$  is the difference in reflection amplitude between spin-up and spin-down electrons in the well. For a more detailed description of the reflection amplitudes, see Refs. 6, 5, and 11. From now on we will assume that there is only one extremal spanning vector ( $Q$ ) on the Fermi surface in the direction that we are investigating. In Fig. 1, a spanning vector is displayed on a cut through the  $\text{Cu}_{0.7}\text{Pd}_{0.3}$  Fermi surface. The generalized Fermi surface radius is calculated by using such spanning vectors in a centered difference approximation of Eq. (3) where the coordinate system is rotated so that  $k_x$  and  $k_y$  are perpendicular to the  $(110)$  direction.

One could expect that the theory breaks down in case of an alloy spacer but as showed in Refs. 14 and 17 the effect of an alloy spacer is an additional exponential damping factor to the formula for the MIC so that

$$J_\infty^{\text{alloy}}(N) = J_\infty(N) e^{-N/\Lambda}. \quad (4)$$

The characteristic length  $\Lambda$  is given by

$$\frac{1}{\Lambda} = \frac{1}{\lambda^+} - \frac{1}{\lambda^-}, \quad (5)$$

where  $\lambda^{+(-)}$  are the mean-free paths in the direction of growth at the two edges of the Fermi surface. In our case we have a symmetric, single sheet Fermi surface so that the condition  $\lambda^+ = -\lambda^-$  is fulfilled and the characteristic length can be calculated as  $\Lambda = (\lambda^+)/2$ . The mean-free paths are calculated as  $1/\lambda = \delta$ , where  $\delta$  is the half-width of the Fermi surface as illustrated in Fig. 2.

For the calculation of the Fermi surface half-widths, the Bloch spectral function

$$A^\sigma(\mathbf{k}, E) = -\frac{1}{\pi} \text{Im Tr } G^\sigma(\mathbf{k}, E) \quad (6)$$

from the Greens function of spin  $\sigma$ , wave vector  $\mathbf{k}$ , and energy  $E$  was evaluated at the Fermi energy  $E_F$ . Since we are

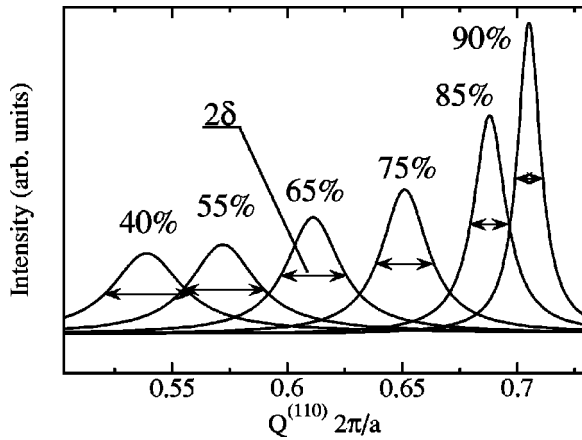


FIG. 2. The Bloch spectral function along the line  $\Gamma$ - $\Delta$ - $X$  for some of the calculated concentrations. The widths for each concentration ( $2\delta$ ) are indicated by the horizontal arrows.

only interested in the behavior along the  $[110]$  direction, we need not to perform the calculation in the full Brillouin zone but restrict the values of  $\mathbf{k}$  to the  $\Gamma$ - $\Delta$ - $X$  line.

### III. RESULTS

#### A. Magnetic moments

The magnetic moments of the interface Fe layer is about  $2.9 \mu_B$  for the 40% Cu systems and decreases linearly with concentration to  $2.6 \mu_B$  for the 90% Cu cases. This is mainly a volume effect since the global volume decreases linearly over the concentration range. For each Cu concentration, the change in moment of the interface Fe is very small when the spacer thickness is varied. In the spacer, the interface Pd atoms have a moment of  $0.25 \mu_B$  for the 40% Cu system and  $0.18 \mu_B$  for the 90% Cu case. The Cu atoms always have a

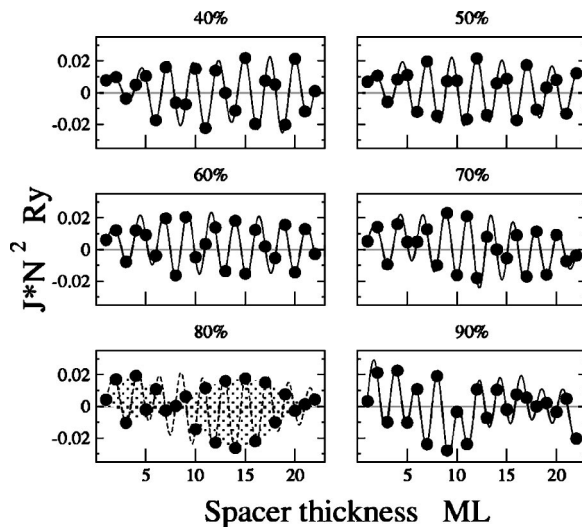


FIG. 3. The MIC as function of spacer thickness for all the Cu concentrations considered (circles). The solid lines are the Fourier backtransforms and they serve as a guide to the eye. The aliasing phenomena is visible for concentrations over 55%. The occurrence of a second, longer period is visible in the 90% case.

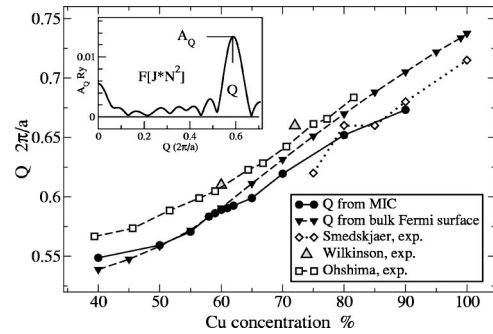


FIG. 4. The nesting vector as obtained by a direct calculation of the bulk Fermi surface and as calculated from a Fourier transform of the MIC. The direction is  $(110)$ . Several experimental results are included for comparison: Smedskjaer,<sup>29</sup> Wilkinson,<sup>21</sup> and Ohshima.<sup>1</sup> The inset shows an example of a raw data Fourier transform of the MIC for 60% Cu and how the values for the amplitude ( $A_Q$ ) and nesting vector ( $Q$ ) are obtained.

very low moment, less than  $0.05 \mu_B$ . The layer-resolved magnetic moment in the spacer averaged over the Cu and Pd atoms always decays to zero within 4 ML from the Fe interface.

#### B. Magnetic interlayer coupling

In Fig. 3 we have plotted the MIC for some of the Cu concentrations considered. In order to make the small oscillations visible, the amplitudes are multiplied by the square of the spacer thickness. We can see that the periods of the oscillations are between 2 and 3 ML and that no additional damping to the amplitudes is evident. There is also an obvious aliasing effect in the 80% case where the “beat” of the oscillation comes from the fact that the period is close to 2 ML and thus the frequency is close to the Nyquist frequency.<sup>30</sup> For the 80% case, the beat is shown through shading, but the effect is present for concentrations down to 55% and we believe that this phenomena is partly responsible for the uncertainty in the Fourier analysis performed later. In the 90% case there is also a new period that appears and this can be seen from the “wavy” form of the MIC. Further processing of the data is not possible without the aid of Fourier analysis and in the following, we will extract information from the Fourier spectra of the data in Fig. 3.

#### C. Nesting vector

First we investigate the change in Fermi surface nesting vector as function of concentration. In Fig. 4 we have plotted the Fermi surface spanning vectors in the interval  $0.4 \leq x \leq 0.9$  as obtained both directly from the Fermi surface calculation and from the Fourier transform of the MIC as function of spacer thickness. The Fourier transforms always showed one single distinct peak and the  $q$  vector for the peak could easily be obtained. A representative Fourier transform for  $x=0.6$  is displayed in the inset. Although some of the layer thicknesses that were used in the Fourier transform clearly are not in the asymptotic region we still get a very good agreement with the nesting vectors from the bulk cal-

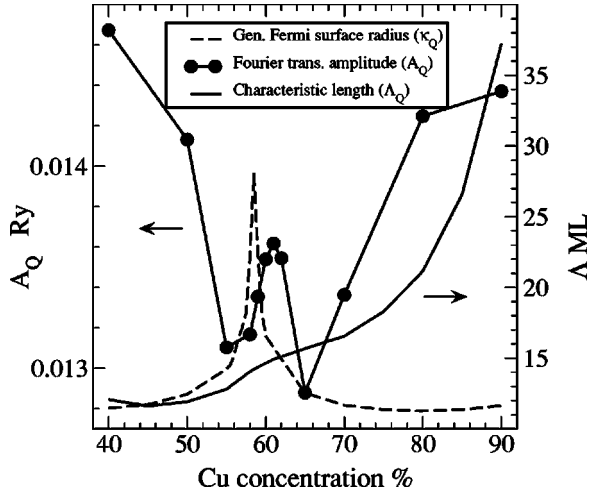


FIG. 5. The amplitude of the largest Fourier transform peak of the MIC for each concentration together with the characteristic lengths and the Fermi surface curvature as calculated from Eq. (3) (arbitrary units).

culations. We can see that the two theoretical curves agree within 5% for all concentrations which indicates that the Fermi surface is well defined in the multilayer system despite the fact that the symmetry is broken in the direction of growth. The spanning vector increases from  $\sim 0.55$  to  $\sim 0.67$  within the considered concentration interval which translates into a period decrease of the MIC from  $\sim 2.6$  to  $\sim 2.1$  ML, respectively. For comparison, experimentally obtained spanning vectors are also plotted, and the agreement is very good.

It is noteworthy that in our bulk calculation of Fe, we see a transition from a high-spin state to an intermediate-spin state where the magnetic moment changes from  $\sim 2.5\mu_B$  to  $\sim 1.6\mu_B$  when the lattice parameter is decreased below  $3.61 \text{ \AA}$ . This implies that we have to limit our investigation to a concentration interval below  $x=0.9$  in order to avoid the effect of this transition in Fe on the MIC.

#### D. Amplitude

In this section we discuss the results obtained for the amplitudes associated with the spanning vectors shown in the previous section. In Fig. 5 we show the amplitude as calculated from the maximum of the Fourier transform for each Cu concentration. This means that the value of  $A_Q$  is the strength of the prefactor in Eq. (2) for the nesting vector ( $Q$ ) provided that the coupling is proportional to  $N^{-2}$ . As will be clear in the discussion about decay later, it is at least very close to this value. Also shown in the figure is the generalized Fermi surface radius and the characteristic length (which are the two bulk properties that are defined by the radius associated with the curvature of the Fermi surface and the inverse of the disorder-induced damping). It is worth noting here that a change in Fermi surface curvature does not generally affect the phase of the MIC unless the nesting region changes between convex, concave or a saddle point.<sup>11</sup> The well-pronounced peak in the amplitude at  $x=0.61$  is located in a global minimum of the coupling which is in agree-

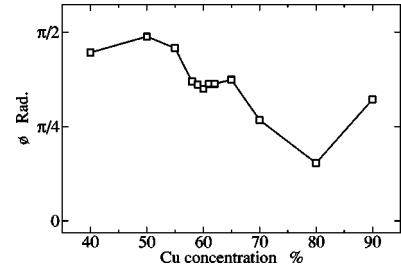


FIG. 6. The phase shift of the oscillation as calculated by  $\phi = \arctan[\text{Im}(F)/\text{Re}(F)]$  and shifted back to the interval  $0 \leq \phi \leq \pi$ .

ment with an increased characteristic length for concentrations to the right of the peak. The amplitude should, however, have a global minimum at 50% Cu if only the characteristic length is considered, but in this alloy the  $d$  band of Pd is intersecting the Fermi energy for concentrations below 50%<sup>31</sup> and we believe this changes the magnetic properties of the spacer, thus having a considerable effect on the MIC.<sup>32</sup> We have also noted that the Fourier transforms change somewhat depending on how many spacer thicknesses that are taken into account. For example if we exclude the small spacer thicknesses with  $\{1-3\}$  ML CuPd and do the transformation on MIC datasets with  $\{4-22\}$  ML we see a small shift in the  $A_Q$  peak positions. However, the peak in  $A_Q$  does not change position by more than  $\pm 1$  on the concentration axis if the number of points is varied. This means that despite not being in the asymptotic region, the effect of Fermi surface nesting is clearly visible.

There are no experimental data concerning the MIC for systems with a CuPd alloy as a spacer and the only investigation of the Fermi surface nesting is that of Wilkinson<sup>21</sup> by positron annihilation. From that work, a crude estimate of the change in nesting may be obtained by comparing the number of measured nesting vectors from the total histograms of the  $\text{Cu}_{60}\text{Pd}_{40}$  and  $\text{Cu}_{72}\text{Pd}_{28}$  measured Fermi surfaces, which is a change of about 75%. The change in MIC amplitude in our calculation between adjacent concentrations with a large difference in amplitude is about 6%. To make a direct experiment on the MIC in this system would probably be a delicate task but the calculated change in amplitude is in principal not beyond experimental detection. We have calculated the MIC by assuming semi-infinite Fe layers in the fcc structure for computational reasons but the effect should also be seen in a system with embedded Fe or Co layers that could adapt to the fcc structure of the CuPd alloy. Whether the fabrication of such multilayers is possible is, at least to our knowledge, an open question.

#### E. Phase

As explained in the general theory for a pure metal spacer in Ref. 11, there should be a phase shift of the MIC associated with a change in the spacer Fermi surface curvature.

In our case, the neighborhood around the nesting vector  $Q$  changes from a minimum to a saddle point when the Cu concentration is changed from 40% to 90%. In order to investigate such a phase shift in our calculation, we have calculated the phase ( $\phi$ ) of the oscillation  $[J(N)]$  from the Fou-

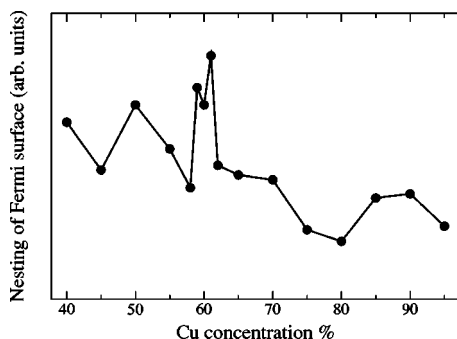


FIG. 7. The normalized number of vectors that take part in the nesting in the [110] direction.

rier transform  $[F(J*N^2)]$  by  $\phi = \arctan[\text{Im}(F)/\text{Re}(F)]$  and the result is shown in Fig. 6.

It is clearly evident that our phase changes continuously with concentration and does not show any abrupt changes as might be expected. An explanation may be that the phase is more sensitive to the change in band matching at the interfaces as the concentration is varied than to the change in Fermi surface curvature. Experimental studies of the phase as function of impurity concentration in the magnetic layer argue that the large observed phase change is due to the altered band matching at the interfaces.<sup>33</sup> In the alloy spacer, the Fermi surface is also not as well defined as in a pure metal (cf. Fig. 2) and the diffuseness may then be responsible for a smearing of the phase shift over a much broader concentration range. There may also be other effects that influence the phase such as the electronic topological transitions of the Fermi surface at 50% and 63% Cu<sup>31</sup> and the aliasing effect due to the discrete monolayer sampling of the MIC.

## IV. DISCUSSION

### A. Nesting from bulk Fermi surface

In order to investigate the nesting from the bulk Fermi surface we have adopted the spanning vector counting method suggested by Wilkinson.<sup>21</sup> In order to do so, we calculated the spectral function in the full Brillouin zone according to Eq. (6) on a grid of  $(64 \times 64 \times 64)$   $k$  points. The spectral function was then further interpolated to a  $120 \times 120 \times 120$  mesh. This mesh was used to construct an isosurface for a given intensity cut of the spectral function. This value was chosen as the highest value possible that still resulted in a continuous surface. Since the isosurface was constructed from the spectral function, it consisted of two separate sheets, but the distance between those sheets was minimized due to the choice of the intensity cut and tests were made to ensure no double peaks when the nesting check was calculated. After this procedure the number of points on the Fermi surface was about 70 000.

We then created a histogram of vectors connecting two points on this surface along a given direction, in our case [110]. This histogram then showed a peak for the vector length that is most frequently represented on our Fermi surface.

The discrete representation of the Fermi surface and the rounding error when calculating the length of the vectors with this method resulted in rough histograms that were smoothed by convolution with a Gaussian function. The intensity of the histograms was also normalized with the number of points on the Fermi surface in order to compare intensities of different concentrations.

In Fig. 7 we have plotted the intensity maximum of the histogram divided by the total number of points on the Fermi surface. It is clear that there is a peak for concentrations around 61%. Compared to the maximum of the generalized curvature there is a difference of about 3 units on the concentration axis and the result agrees perfectly with the maximum amplitude of the MIC.

The histogram in Fig. 7 has an unexpected nonmonotonic behavior. We believe that the reason is that the Fermi surfaces were calculated on a grid and thereby the spatial resolution becomes quite low for computer memory reasons. The sparse grid is then responsible for the “jagged” appearance of the figure. Although the figure has this drawback, the peak at 60% is still visible and distinguishable from the “noise.”

### B. Amplitude

The amplitude of the MIC is a much more complicated quantity to calculate compared to the period of the oscillation. From Eq. (2) we can see that the amplitude, even in the ideal model case, depends on a number of factors. In this discussion we will assume that the Fermi velocity term ( $v$ ) is constant or at least very slowly varying over the concentration interval. An estimation of the change in Fermi velocity may be performed by inspecting the bulk band structure of Cu and Pd for the [110] direction and taking the slope of the band at the Fermi level. Our estimation gives a change in Fermi velocity of no more than 4% over our concentration interval.

The reflection coefficients are much harder to estimate. They may, in general, vary irregularly with concentration and the quadratic contribution to the amplitude is strong. A quantitative investigation of the variation of the reflection coefficients with concentration is a comprehensive task and is beyond the scope of this paper. Calculations of reflection coefficients were made in Refs. 34–36. However, above  $x = 0.55$ , the  $d$  band of Pd is already below the Fermi energy and the variation in band matching (at least at the Fermi level) is only from the  $s$  band. The  $s$  band is not changing very much between Cu and Pd so we assume that the band matching, which gives the reflection coefficients, does not change very much in the interval. We therefore assume that the reflection coefficients will not affect the trend of the amplitudes more than in a monotonic way.

The remaining quantities that affect the coupling are the generalized Fermi surface radius and characteristic length. They were calculated from the Fermi surfaces of the corresponding CuPd bulk alloys and since we are not completely in the asymptotic region, the comparison to the amplitudes from the full multilayer calculations is not strictly justified. However, the concentrations where  $\kappa$  diverges and the amplitude has a maximum are very close and we argue that the

small discrepancy is partly due to this preasymptotic effect.

Close to  $x=0.58$ , the Fermi surface is perfectly flat in one  $k_{\parallel}$  direction and does thus show nesting along a line. The result is that Eq. (3) breaks down and diverges. At the pole  $\kappa$  changes sign which reflects the change from a minimum to a saddle point around the nesting caliper. In Fig. 5, therefore, the absolute value of  $\kappa$  is displayed (in arbitrary units).

### C. Decay

The characteristic length that was calculated within this model is displayed in Fig. 5. In order to check for the extra decay that is associated with the characteristic length, we have also performed a least squares fit of exponentially decaying functions to the MIC. From that analysis, we have concluded that there is no decay, apart from the assumed  $1/N^2$  decay, in the calculated MIC on the order of the estimations in Fig. 5. This indicates that the disorder induced decay is not easily observed in the studied spacer thickness range.

The lack of damping is also evident in two cases in Ref. 18, Fig. 3 where the MIC was calculated for  $\text{Cu}_{0.5}\text{Au}_{0.5}$ ,  $\text{Cu}_{0.75}\text{Ni}_{0.25}$  and  $\text{Cu}_{0.5}\text{Zn}_{0.5}$ . We have calculated the characteristic lengths for these three alloys in the same way as for our CuPd case to be 23, 87, and 23 ML, respectively. In Ref. 18, there is only clear exponential damping for the CuZn case although the damping is the same for the CuAu alloy. It is then very interesting to examine Ref. 17 where the same authors present an extended calculation of the CuAu system [Fig. 4(e)] where they double the number of calculated spacer layers from 45 to 90 ML, the damping then appearing for thicknesses over 45 ML. An estimate of the exponential damping from the figures presented gives the characteristic length for the CuAu case to be  $\sim 76$  ML whereas the same property for CuZn becomes  $\sim 25$  ML which agrees with our calculated characteristic length from the Fermi surface. Thus, the damping term may not be as simple as previously thought and may contain some unknown, element specific, prefactor which would explain the appearance of the damping in the CuAu case. It may also be that, for some cases, the damping cannot be calculated from a single point on the Fermi surface by using the Bloch spectral function within the CPA.

Since we calculate the characteristic lengths from the point where the nesting vector touches the Fermi surface we neglect contributions from all other vectors when the Fermi surface is flat. In our case this may be a large source of error since we are investigating a system with substantial nesting. It is not known how all factors in Eq. (2) converge with  $k$

points for total energy calculations and we speculate that the exponential damping term may be very hard to converge.

## V. CONCLUSIONS

The amplitude maximum of the MIC and the maximum nesting strength show a remarkable agreement. We thus conclude that the MIC is affected by the nesting in a way that is well described by the RKKY model. However, the agreement between the divergence of the generalized Fermi surface radius and the peak in MIC is not perfect and an analysis of the nesting of the bulk alloy Fermi surfaces show that the true nesting peak and the divergence in Fermi surface radius do not occur at exactly the same concentration.

The expected phase shift that is associated with the divergence of the generalized Fermi surface curvature is not seen in our calculations but the phase changes continuously over the concentration range. We expect that the phase shift should be seen if the calculation was extended further into the asymptotic region. We also do not see the anticipated disorder-induced decay of the amplitude and the comparison to calculations by Bruno and Kudrnovsky<sup>17,18</sup> indicates that this decay may be visible only for very large systems ( $N > 45$ ).

The increase in the calculated amplitude is about 10% and would in principle be measurable in an experiment if the interface quality is good enough.

## VI. SUMMARY

We have performed full *ab initio*, total energy calculations of the MIC in  $\text{Fe}/\text{Cu}_x\text{Pd}_{1-x}/\text{Fe}$  random alloy systems for  $0.4 \leq x \leq 0.9$  and spacer thicknesses of 1–22 ML. At the concentration  $x \sim 0.6$  we see a large effect on the amplitude from Fermi surface nesting. We have also investigated the period, phase, and disorder-induced decay of the MIC. The small difference in predicted amplitude maximum from bulk Fermi surface calculations is argued to originate mainly from preasymptotic effects. The results give important information on the applicability of asymptotic models for the MIC.

## ACKNOWLEDGMENTS

This work was supported from the Swedish Research Council (VR), the Swedish Foundation for Strategic Research (SSF), and the European Network for Computational Magneto-electronics. S.B.D. is supported by the Royal Society (UK). Discussions with Nektarios Lathiotakis and Josef Kudrnovsky are gratefully acknowledged. Special thanks also go to B. Lizárraga for strong support.

\*Electronic address: erik.holmstrom@fysik.uu.se

<sup>1</sup>K. Ohshima and D. Watanabe, *Acta Crystallogr., Sect. A: Cryst. Phys., Diffir., Theor. Gen. Crystallogr.* **A29**, 520 (1973).

<sup>2</sup>C. Y. You, C. H. Sowers, A. Inomata, J. S. Jiang, S. D. Bader, and D. D. Koelling, *J. Appl. Phys.* **85**, 5889 (1999).

<sup>3</sup>M. T. Johnson, S. T. Purcell, N. W. E. McGee, R. Coehoorn, J. aan de Stegge, and W. Hoving, *Phys. Rev. Lett.* **68**, 2688 (1992).

<sup>4</sup>P. J. H. Bloemen, R. van Dalen, W. J. M. de Jonge, M. T. Johnson, and J. aan de Stegge, *J. Appl. Phys.* **73**, 5972 (1993).

- <sup>5</sup>P. Bruno, Phys. Rev. B **52**, 411 (1995).
- <sup>6</sup>M. D. Stiles, Phys. Rev. B **48**, 7238 (1993).
- <sup>7</sup>M. D. Stiles, J. Magn. Magn. Mater. **200**, 322 (1999).
- <sup>8</sup>A. M. N. Niklasson, S. Mirbt, H. L. Skriver, and B. Johansson, Phys. Rev. B **53**, 8509 (1996).
- <sup>9</sup>N. N. Lathiotakis, B. L. Györfy, E. Bruno, B. Ginatempo, and S. P. Parkin, Phys. Rev. Lett. **83**, 215 (1999).
- <sup>10</sup>P. Bruno and C. Chappert, Phys. Rev. Lett. **67**, 1602 (1991).
- <sup>11</sup>P. Bruno and C. Chappert, Phys. Rev. B **46**, 261 (1992).
- <sup>12</sup>S. N. Okuno and K. Inomata, Phys. Rev. Lett. **70**, 1711 (1993).
- <sup>13</sup>J. F. Bobo, L. Hennet, and M. Piecuch, Europhys. Lett. **24**, 139 (1993).
- <sup>14</sup>N. N. Lathiotakis, B. L. Györfy, J. B. Staunton, and B. Újfalussy, J. Magn. Magn. Mater. **185**, 293 (1998).
- <sup>15</sup>N. N. Lathiotakis, B. L. Györfy, and J. B. Staunton, J. Phys.: Condens. Matter **10**, 10357 (1998).
- <sup>16</sup>N. N. Lathiotakis, B. L. Györfy, E. Bruno, and B. Ginatempo, Phys. Rev. B **62**, 9005 (2000).
- <sup>17</sup>P. Bruno, J. Kudrnovsky, V. Drchal, and I. Turek, J. Magn. Magn. Mater. **165**, 128 (1997).
- <sup>18</sup>J. Kudrnovsky, V. Drchal, P. Bruno, I. Turek, and P. Weinberger, Phys. Rev. B **54**, R3738 (1996).
- <sup>19</sup>K. Takanashi, R. Schreiber, I. Mertig, and P. Grünberg, J. Magn. Magn. Mater. **156**, 237 (1996).
- <sup>20</sup>B. L. Györfy and G. M. Stocks, Phys. Rev. Lett. **50**, 374 (1983).
- <sup>21</sup>I. Wilkinson, R. J. Hughes, Z. Major, S. B. Dugdale, M. A. Alam, E. Bruno, B. Ginatempo, and E. S. Giuliano, Phys. Rev. Lett. **87**, 216401 (2001).
- <sup>22</sup>O. Andersen, A. Postnikov, and S. Savrasov, *Applications of Multiple Scattering Theory in Materials Science* (Materials Research Society, Pittsburgh, PA, 1992), Vol. 253, pp. 37–70.
- <sup>23</sup>J. P. Perdew, K. Burke, and M. Ernzerhof, Phys. Rev. Lett. **77**, 3865 (1996).
- <sup>24</sup>H. L. Skriver and N. M. Rosengaard, Phys. Rev. B **43**, 9538 (1991).
- <sup>25</sup>P. Soven, Phys. Rev. **156**, 809 (1967).
- <sup>26</sup>I. A. Abrikosov and H. L. Skriver, Phys. Rev. B **47**, 16 532 (1993).
- <sup>27</sup>B. L. Györfy, Phys. Rev. B **5**, 2382 (1972).
- <sup>28</sup>S. Dugdale, unpublished fully relativistic KKR calculations.
- <sup>29</sup>L. C. Smedskjaer, R. Benedek, R. W. Siegel, D. G. Legnini, M. D. Stahulak, and A. Bansil, Phys. Rev. Lett. **59**, 2479 (1987).
- <sup>30</sup>H. Nyquist, Trans. A.I.E.E. **47**, 617 (1928).
- <sup>31</sup>E. Bruno, B. Ginatempo, and E. S. Giuliano, Phys. Rev. B **63**, 174107 (2001).
- <sup>32</sup>E. Holmström, L. Nordström, and A. M. N. Niklasson, Phys. Rev. B **67**, 184403 (2003).
- <sup>33</sup>U. Ebels, R. L. Stamps, L. Zhou, P. E. Wigen, K. Ounadjela, J. Gregg, J. Morkowski, and A. Szajek, Phys. Rev. B **58**, 6367 (1998).
- <sup>34</sup>M. D. Stiles, J. Appl. Phys. **79**, 5805 (1996).
- <sup>35</sup>K. Wildberger, R. Zeller, P. H. Dederichs, J. Kudrnovsky, and P. Weinberger, Phys. Rev. B **58**, 13 721 (1998).
- <sup>36</sup>I. Riedel, P. Zahn, and I. Mertig, Phys. Rev. B **63**, 195403 (2001).